PHYSICAL REVIEW B VOLUME 22, NUMBER 4 15 AUGUST 1980

Soliton excitations in polyacetylene

W. P. Su,* J. R. Schrieffer,* and A. J. Heeger
Department of Physics, University of Pennsylvania, Philadelphia, Pennsylvania 19174
(Received 3 December 1979)

A theoretical analysis of the excitation spectrum of long-chain polyenes is presented. Because of the twofold degeneracy of the ground state of the dimerized chain, elementary excitations corresponding to topological solitons are obtained. The solitons can have three charge states $Q=0, \pm e$. The neutral soliton has spin one-half while the charged solitons have spin zero. One electronic state is localized at the gap center for each soliton or antisoliton present. The soliton's energy of formation, length, mass, activation energy for motion, and electronic properties are calculated. These results are compared with experiment.

I. INTRODUCTION

Because of the degenerate ground state of the bond-alternated polyene chain, one expects excitations to exist in the form of a topological soliton, or moving domain wall. In an earlier paper,[1] we suggested the possibility of such soliton formation in the conjugated organic polymer $(CH)_x$, polyacetylene, and we outlined some of the implied experimental consequences. Related theoretical studies have been carried out in a Ginzburg-Landau[2] scheme as well as in a continuum approximation.[3–5]

Magnetic-resonance studies of undoped *trans*-$(CH)_x$ have shown the existence of highly mobile neutral magnetic defects in the polymer chain.[6–10] Since a charge neutral soliton in a long-chain polyene would have an unpaired spin localized in the wall, it was suggested that the motionally narrowed spin resonance might arise from bond-alternation domain walls induced upon isomerization. Moreover, analysis of the transport[11] and magnetic properties[8] in lightly doped samples led to the suggestion that doping may proceed through formation of charged domain walls. Thus, the concept of soliton formation and the detailed evaluation of properties are of direct interest to the continuing development of this novel class of conducting polymers.

Our theory assumes the existence of bond alternation along the polymer chain (i.e., alternating "single" and "double" bonds) and relatively weak interchain coupling (i.e., quasi-one-dimensional behavior). There is experimental evidence that both these assumptions are valid in $(CH)_x$. Raman studies[12,13] have detected the splitting of the carbon-carbon bond stretch vibrations resulting from bond alternation consistent with the normal mode analysis.[14] Weak interchain coupling is suggested by the observation of considerable anisotropy in physical properties after polymer orientation.[15] Moreover, recent nuclear-magnetic-resonance studies have[16] demonstrated one-dimensional electronic spin diffusion in the polymer, both undoped and heavily doped.

In this paper we present a detailed theory of soliton formation in long-chain polyenes in the one-electron approximation. The model Hamiltonian is described in Sec. II and solved for the perfect dimerized chain in Sec. III. Soliton excitations and their properties are derived in Sec. IV, and doping effects are considered briefly in Sec. V. Section VI includes a brief comparison with experimental results.

II. MODEL HAMILTONIAN

To simplify our description of $(CH)_x$, we assume, as described above, that to lowest order one can neglect interchain electron hybridization. Also, we assume that the σ electrons can be treated in the adiabatic approximation since the gap between the σ bonding and antibonding states is large (~ 10 eV) compared to the phonon and soliton energies ($\lesssim 0.5$ eV). Furthermore, since we are interested primarily in the dimerization structure of *trans*-$(CH)_x$, we treat only that configuration coordinate u_n for each CH group n which describes translation of the group along the symmetry axis (x) of the chain, as shown in Fig. 1. For the structure shown in Fig. 1(a) $u_n < 0$, while u_{n+1} and $u_{n-1} > 0$, leading to a short ("double") bond between groups $n-1$ and n, and a long ("single") bond between n and $n+1$. These displacements have the reverse signs if double and single bonds are interchanged, as in Fig. 1(b). Let a be the equilibrium spacing between the x coordinates of successive CH groups in the undimerized structure (i.e., all bond orders equal to 1.5). a is approximately $1.40 \times \sqrt{3}/2$ Å $= 1.22$ Å. Because of symmetry, the remaining five coordinates for each CH group are not coupled into the dimerization structure to first order in phonon coordinates and will be neglected.

Since the change of bond length due to dimeriza-

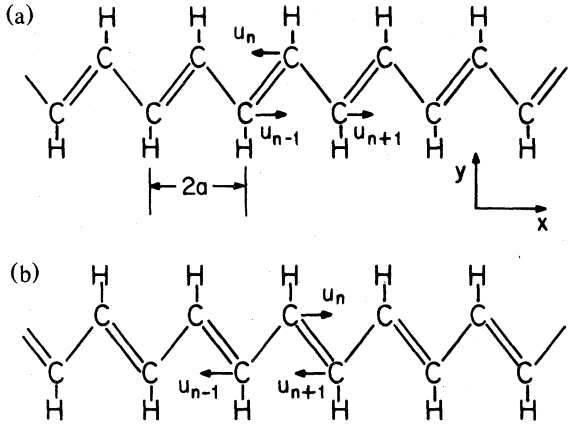

FIG. 1. Perfectly dimerized *trans*-polyacetylene showing the dimerization coordinate u_n for the two degenerate ground states: A phase [Fig. 1(a)] and B phase [Fig. 1(b)].

tion is small, of order 0.08 Å, we assume that the σ bonding energy can be expanded to second order about the undimerized state,

$$E_\sigma = \frac{1}{2}\sum_n K(u_{n+1}-u_n)^2 \ . \tag{2.1}$$

where K is the effective σ spring constant.

We assume the π electrons (p_z orbitals) can be treated in the tight-binding or Hückel-type approximation with a hopping integral $t_{n+1,n}$ which can be expanded to first order about the undimerized state

$$t_{n+1,n} = t_0 - \alpha(u_{n+1}-u_n) \ . \tag{2.2}$$

t_0 is the hopping integral for the undimerized chain and α is the electron-lattice displacement (phonon) coupling constant. Model calculations[17,19] indicate that this linear approximation is valid since the bond-length changes are small. A sketch of $t_{n+1,n}$ is shown in Fig. 2. We note that Eq. (2.2) is the standard form of the electron-phonon coupling in metals.

Finally, the kinetic energy of nuclear motion is given by

$$E_k = \frac{1}{2}\sum_n M\dot{u}_n^2 \ , \tag{2.3}$$

where M is the total mass of the CH group. The model Hamiltonian is the sum of these energies

$$H = -\sum_{ns} t_{n+1,n}(c^\dagger_{n+1,s}c_{ns} + c^\dagger_{ns}c_{n+1,s}) + \frac{1}{2}\sum_n K(u_{n+1}-u_n)^2 + \frac{1}{2}\sum_n M\dot{u}_n^2 \ , \tag{2.4}$$

where $c^\dagger_{ns}$ and c_{ns} create and destroy π electrons of spin $s(\pm\frac{1}{2})$ on the nth CH group. The $c^\dagger$ and c satisfy Fermi anticommutation relations while u_n and $p_n = M\dot{u}_n$ satisfy canonical commutation relations

$$[p_n, u_{n'}] = \delta_{nn'}\hbar/i \ . \tag{2.5}$$

We note that *cis*-$(CH)_x$ can be treated in a similar manner using the configuration coordinate u_n shown in Fig. 3. For the pattern shown in Fig. 3(a), u_n and u_{n+2} are negative and u_{n-1} and u_{n+1} are positive, while the signs are reversed for the configuration in Fig. 3(b).

Missing from H are the explicit Coulomb interactions between π electrons. They are partially included by using screened values of t_0 and α. We also treat Coulomb interactions between the charged soliton and impurities. However, if the π-π Coulomb interactions are very strong, our approach is invalid and one should start from the "large-U" limit for the π electrons.

Finally, we note that H should be supplemented with the constraint of fixed total length of the chain, since we assume that a is the equilibrium lattice spacing of the undimerized, including π bonding.

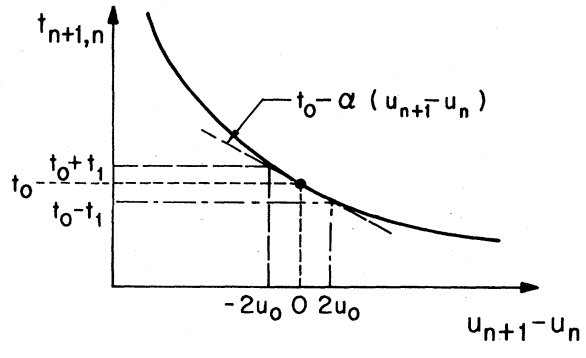

FIG. 2. Nearest-neighbor hopping integral as a function of the dimerization coordinate difference. The undimerized chain has $u_{n+1}-u_n=0$, while this difference is equal to $2u_0$ and $-2u_0$ for a single and a double bond, respectively.

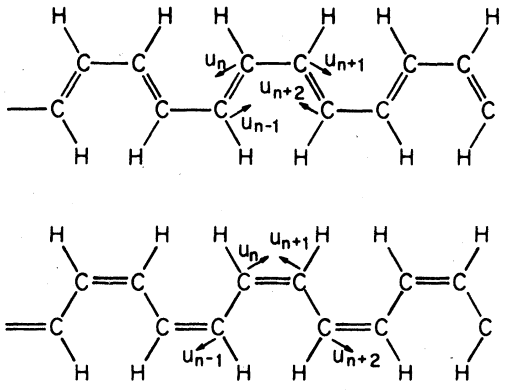

FIG. 3. Two dimerization structures for *cis*-polyacetylene, the dimerization coordinates are perpendicular to the C–H bonds, as shown. The A and B structures are not degenerate in energy as they are for the *trans* phase.

III. PERFECTLY DIMERIZED CHAIN

We begin by investigating the perfectly dimerized chain in the Born-Oppenheimer approximation, where the configuration coordinates u_n are constrained to be

$$u_n = (-1)^n u \quad . \tag{3.1}$$

The kinetic energy E_M will be treated later. By evaluating the ground-state energy as a function of u, one can determine the values of the displacement amplitude u which minimize the total energy E_0. By symmetry, if u_0 minimized E_0, so does $-u_0$. Hence we expect a twofold degenerate ground state corresponding to the two-bondings configurations shown in Figs. 1(a) and 1(b).

For fixed u, the first two terms of Eq. (2.4) are

$$H^d(u) = -\sum_{ns} [t_0 + (-1)^n 2\alpha u] \times (c^{\dagger}_{n+1,s} c_{ns} + c^{\dagger}_{ns} c_{n+1,s}) + 2NKu^2 \quad . \tag{3.2}$$

Since the hopping potential is periodic with a period $2a$, we use a reduced-zone scheme with zone boundaries at $\pm\pi/2a$. In Fig. 4 the zero-order ($u = 0$) bands are shown, where,

$$E_k^{0v} = -2t_0 \cos ka = -\epsilon_k \quad ,$$
$$E_k^{0c} = +2t_0 \cos ka = \epsilon_k \quad . \tag{3.3}$$

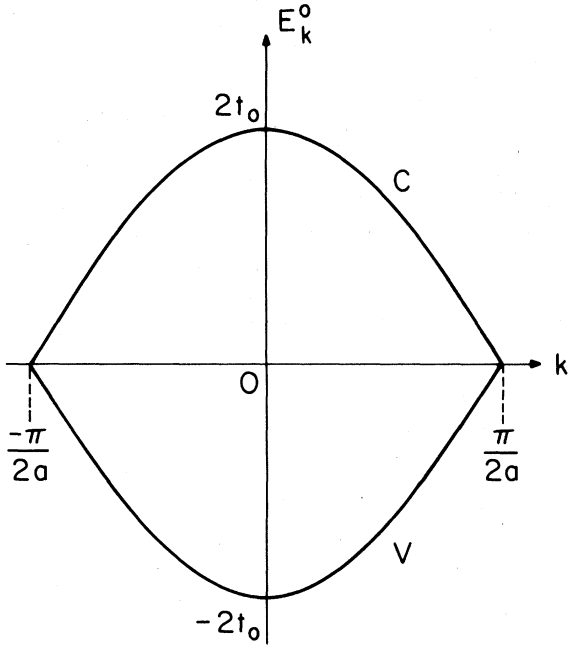

FIG. 4. π bands for undimerized *trans*-$(CH)_x$ with a zone scheme for a unit cell having two CH groups. When dimerization is included, gaps occur at $k = \pm\pi/2a$, with C and V becoming the conduction and valence bands of a semiconductor.

The conduction- and valence-band states are given by

$$\chi_k^v = \frac{1}{\sqrt{N}} \sum_n e^{ikan} \phi_n \quad . \tag{3.4a}$$

$$\chi_k^c = \frac{1}{\sqrt{N}} \sum_n e^{ikan} (-1)^n \phi_n \quad . \tag{3.4b}$$

where ϕ_n is the π orbital on the nth group. We use periodic boundary conditions on a chain of N CH groups. The chain length is $L = Na$. The operators c_k^v and c_k^c for the zero-order bands are related to the operators c_{ns} by

$$c_{ks}^v = \frac{1}{\sqrt{N}} \sum_n e^{ikan} c_{ns} \quad . \tag{3.5a}$$

$$c_{ks}^c = \frac{1}{\sqrt{N}} \sum_n e^{ikan} (-1)^n c_{ns} \quad . \tag{3.5b}$$

By inverting these transformations H^d can be expressed in the k representation

$$H^d = \sum_{ks} [\epsilon_k (c_{ks}^{c+} c_{ks}^c - c_{ks}^{v+} c_{ks}^v) + 4\alpha u \sin ka \, (c_{ks}^{c+} c_{ks}^v + c_{ks}^{v+} c_{ks}^c)] + 2NKu^2 \quad . \tag{3.6}$$

Finally, H^d can be brought to diagonal form by defining operators

$$a_{ks}^v = \alpha_k c_{ks}^v + \beta_k c_{ks}^c \quad , \tag{3.7a}$$

$$a_{ks}^c = \alpha_k^* c_{ks}^c - \beta_k^* c_{ks}^v \quad , \tag{3.7b}$$

where

$$|\alpha_k|^2 + |\beta_k|^2 = 1 \quad . \tag{3.8}$$

By inverting Eq. (3.7) and requiring that H^d be diagonal in the a operators, one finds

$$H^d = \sum_{ks} E_k (n_{ks}^c - n_{ks}^v) + 2NKu^2 \quad , \tag{3.9}$$

where

$$E_k = (\epsilon_k^2 + \Delta_k^2)^{1/2} \tag{3.10}$$

and the gap parameter Δ_k is defined by

$$\Delta_k = 4\alpha u \sin ka \quad , \tag{3.11}$$

with $n = a^+ a$ being the occupation number operator, as usual. The transformation coefficients, for α_k = real positive, are given by

$$\alpha_k = \left[\frac{1}{2}\left(1 + \frac{\epsilon_k}{E_k}\right)\right]^{1/2} \quad , \tag{3.12a}$$

$$\beta_k = \left[\frac{1}{2}\left(1 - \frac{\epsilon_k}{E_k}\right)\right]^{1/2} \mathrm{sgn} k \quad . \tag{3.12b}$$

Thus, the single-particle energy eigenstates of the

perfectly dimerized lattice are

$$\psi_k^v = \left[\frac{1}{2}\left(1+\frac{\epsilon_k}{E_k}\right)\right]^{1/2} \chi_k^v + \mathrm{sgn}k\left[\frac{1}{2}\left(1-\frac{\epsilon_k}{E_k}\right)\right]^{1/2} \chi_k^c \ , \tag{3.13a}$$

$$\psi_k^c = \left[\frac{1}{2}\left(1+\frac{\epsilon_k}{E_k}\right)\right]^{1/2} \chi_k^c - \mathrm{sgn}k\left[\frac{1}{2}\left(1-\frac{\epsilon_k}{E_k}\right)\right]^{1/2} \chi_k^v \ , \tag{3.13b}$$

with eigenvalues

$$E_k^v = -E_k, \quad E_k^c = +E_k \ . \tag{3.14}$$

Phases are chosen so that $\psi_k^{v,c} \to \chi_k^{v,c}$ as $\Delta_k \to 0$.

The ground state of the chain for exactly one π electron per atom on average is given as a function of u by Eq. (3.9) where $n_{ks}^v = 1$ and $n_{ks}^c = 0$. One has

$$E_0(u) = -2\sum_k E_k + 2NKu^2 \ , \tag{3.15}$$

where k is summed over the first Brillouin zone of the dimerized lattice $-\pi/2a \le k \le \pi/2a$ with the two terms in Eq. (3.15) corresponding to the π and σ energies. By replacing the sum by an integral, one obtains

$$E_0(u) = -\frac{2L}{\pi}\int_0^{\pi/2a} [(2t_0\cos ka)^2 + (4\alpha u \sin ka)^2]^{1/2} dk + 2NKu^2 \tag{3.16a}$$

$$= -\frac{4Nt_0}{\pi}\int_0^{\pi/2} [1-(1-z^2)\sin^2 ka]^{1/2} dk\, a + 2NKu^2 \tag{3.16b}$$

$$= -\frac{4Nt_0}{\pi} E(1-z^2) + \frac{NKt_0^2 z^2}{2\alpha^2} \ , \tag{3.16c}$$

where $E(1-z^2)$ is the elliptic integral and

$$z = \frac{t_1}{t_0} = \frac{2\alpha u}{t_0} \ . \tag{3.17}$$

For small z,

$$E(1-z^2) \cong 1 + \tfrac{1}{2}(\ln 4/|z| - \tfrac{1}{2})z^2 + \cdots \ . \tag{3.18}$$

Therefore, the π energy is always more negative than the σ energy and $E_0(u)$ has a local maximum at $u = 0$, corresponding to the Peierls theorem. Taking the value[19] $K = 21$ eV/Å^2, the π bandwidths[20] as $W_\pi = 4t_0 = 10$ eV, and choosing α so that E_0 has a minimum when the dimerization gap is $E_G = 4t_1 = 1.40$ eV, we find $E_0(u)$ shown in Fig. 5, with minima at $\pm u_0$ where $u_0 = 0.04$ Å. With this choice of parameters, we find $\alpha = 4.1$ eV/Å, a value comparable to that given by quantum chemical calculations.[17] The bond-length change due to dimerization is $\pm\sqrt{3}\,u_0 = \pm 0.073$ Å, close to the value used by Baughman *et al.*[21] in their calculations. The condensation energy per site in eV is

$$-\frac{E_c}{N} = \frac{1}{N}[E_0(u_0) - E_0(0)] = -0.015 \ . \tag{3.19}$$

The density of states per spin of the perfect dimerized bands is

$$\rho_0(E) = \frac{L}{2\pi|dE_k/dk|} = \begin{cases} (N/\pi)|E|/[(4t_0^2 - E^2)(E^2-\Delta^2)]^{1/2}, & \Delta \le |E| \le 2t_0 \ , \\ 0, \quad \text{otherwise} \ , \end{cases} \tag{3.20}$$

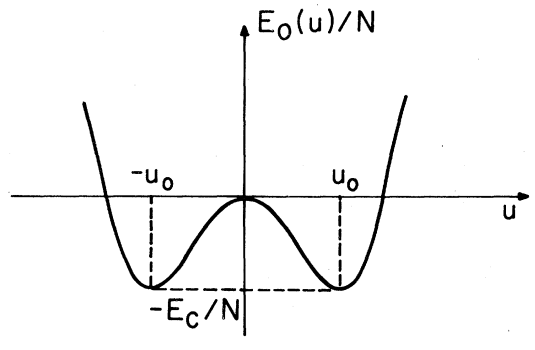

FIG. 5. Born-Oppenheimer energy per CH group plotted as a function of the staggered dimerization coordinate $u = (-1)^n u_n$. The two stable minima correspond to $A(+u_0)$ and $B(-u_0)$ phases.

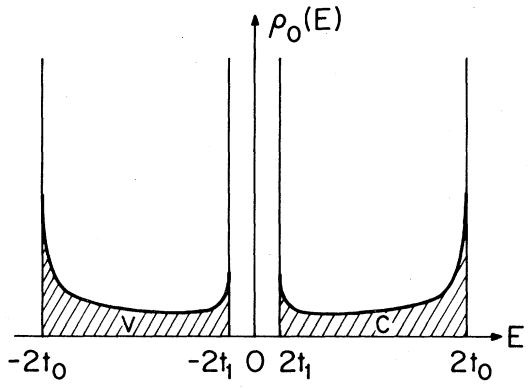

FIG. 6. One-electron density of states for A or B phase *trans*-$(CH)_x$.

where the gap parameter Δ is defined as

$$\Delta \equiv \Delta_{\pi/2a} = 4\alpha u_0 = 2t_1 \ . \tag{3.21}$$

$\rho_0(E)$ is plotted in Fig. 6.

Since our treatment of the soliton requires the Green's function $G^d(\omega)$ for the perfect dimerized lattice, we next derive this quantity. Using the eigenfunction expansion one has

$$G^d_{nn'}(\omega) = \sum_{k,\lambda} \frac{\psi^\lambda_k(n)\psi^{\lambda *}_k(n')}{\omega - E^\lambda_k + i\delta} \ , \tag{3.22}$$

where $\delta = 0^+, 0^-$ for $\lambda = c, v$, respectively, and the wave functions $\psi^\lambda_k(n) = \langle \phi_n | \psi^\lambda_k \rangle$ are given by Eqs. (3.4a) and (3.13a),

$$\psi^v_k(n) = [\alpha_k + i\beta_k(-1)^n] e^{ikan}/\sqrt{N} \ , \tag{3.23a}$$

$$\psi^c_k(n) = [i\alpha_k(-1)^n - \beta_k] e^{ikan}/\sqrt{N} = -i(-1)^n \psi^v_k(n) \ . \tag{3.23b}$$

Thus, combining Eqs. (3.8), (3.22), and (3.23), one has

$$G^d_{nn'}(\omega) = \begin{cases} \dfrac{1}{N}\displaystyle\sum_k \dfrac{2\omega e^{ika(n-n')}}{(\omega+i\delta)^2 - E_k^2}, & n-n' \text{ even} \quad (3.24) \\ -\dfrac{1}{N}\displaystyle\sum_k \dfrac{2E_k[\alpha_k + i\beta_k(-1)^n]^2 e^{ika(n-n')}}{(\omega+i\delta)^2 - E_k^2}, & n-n' \text{ odd.} \quad (3.25) \end{cases}$$

For the diagonal element, one finds

$$G^d_{nn}(\omega) = \begin{cases} \dfrac{-i\omega}{[(4t_0^2 - \omega^2\chi\omega^2 - \Delta^2)]^{1/2}}, & \Delta \le |\omega| \le 2t_0 \\ \dfrac{-\omega}{[(4t_0^2 - \omega^2)(\Delta^2 - \omega^2)]^{1/2}}, & 0 < |\omega| < \Delta \\ \dfrac{\omega}{[(\omega^2 - 4t_0^2)(\omega^2 - \Delta^2)]^{1/2}}, & |\omega| > 2t_0 \ . \end{cases}$$

This expression is consistent with the density-of-states Eq. (3.20) expression since

$$\rho^d(E) = -\frac{\mathrm{sgn}E}{\pi} \sum_n \mathrm{Im} G^d_{nn}(E) \ . \tag{3.26}$$

We note for later use that

$$G^d_{n,n+1}(\omega) = \begin{cases} \dfrac{1}{2(t_1^2 - t_0^2)} \left\{ -(t_0 + t_1) + i\left[t_1 \left(\dfrac{1+B}{1-B} \right)^{1/2} - t_0 \left(\dfrac{1-B}{1+B} \right)^{1/2} \right] \right\}, & 2t_1 \le |\omega| \le 2t_0 \quad (3.27a) \\ \dfrac{1}{2(t_1^2 - t_0^2)} \left[-(t_0 + t_1) + t_1 \left(\dfrac{B+1}{B-1} \right)^{1/2} + t_0 \left(\dfrac{B-1}{B+1} \right)^{1/2} \right], & |\omega| \le 2t_1, \text{ or } |\omega| > 2t_0. \quad (3.27b) \end{cases}$$

where

$$B = \frac{t_0^2 + t_1^2 - \frac{1}{2}\omega^2}{(t_0^2 - t_1^2)}, \quad n \text{ odd} \tag{3.28}$$

and $t_1 = \frac{1}{2}\Delta$, as defined above. Equations (3.27) and (3.28) apply for n odd while the same expressions hold with t_1 replaced by $-t_1$ for n even. As an application of these expressions we calculate the frequency dependence of the optical-absorption rate. In the long-wavelength limit, the dielectric tensor is

$$\epsilon_{jj}(\omega) = 1 + \frac{4\hbar^2\pi n e^2}{m_e^2\omega^2} \sum_k \frac{|\langle \psi^c_k | p_j | \psi^v_k \rangle|^2}{2E_k - \omega + i\delta} \ , \tag{3.29}$$

where n is the π electron density and m_e is the electron mass. For polarization of the electric field along the chain, $j = x$, and assuming next-nearest-neighbor π orbitals do not overlap, one has,

$$\langle \psi^c_k | p_x | \psi^v_k \rangle = i 2\Delta M_x \sin^2 ka / E_k \ , \tag{3.30}$$

where M_x is the dipole matrix element

$$M_x = \frac{\hbar}{i} \int \phi(x,y,z) \frac{\partial}{\partial x} \phi(x+a,y,z)\, d^3r \ . \tag{3.31}$$

Inserting Eq. (3.30) into Eq. (3.29), one finds

$$\mathrm{Im}\epsilon_{xx}(\omega) \propto \begin{cases} \dfrac{[(4t_0)^2 - \omega^2]^{3/2}}{\omega^3(\omega^2 - 4\Delta^2)^{1/2}}, & 2\Delta \le |\omega| \le 4t_0 \\ 0, \quad \text{otherwise} \ . \end{cases} \tag{3.32}$$

This expression is plotted in Fig. 7 in comparison with experiment. The experimental results are obtained from analysis of the inelastic electron scattering data of Ritsko *et al.*[15] on nonoriented $(CH)_x$ films.

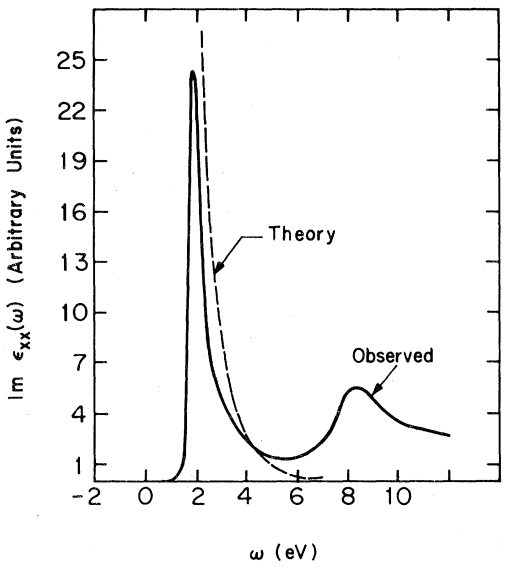

FIG. 7. Infrared absorption plotted as a function of photon energy for undoped *trans*-$(CH)_x$. The experimental results are obtained from analysis of the inelastic electron-scattering data of Ritsko *et al.* (Ref. 15) on nonoriented $(CH)_x$ films.

IV. SOLITON EXCITATION

As we discussed above, the classical ground state of the dimerized chain is twofold degenerate with $u_{0n} = \pm(-1)^n u_0$. Associated with this degeneracy, we expect there to exist an elementary excitation corresponding to a soliton.[22] It is useful to define an order parameter ψ_n associated with any displacement u_n

$$\psi_n = (-1)^n u_n, \quad u_n = (-1)^n \psi_n \ . \tag{4.1}$$

The two ground states are then defined by

$$\psi_{0n} = \begin{cases} -u_0, & A \text{ phase}, \\ u_0, & B \text{ phase}. \end{cases} \tag{4.2}$$

Suppose that ψ_n approaches $-u_0$(A phase) as $n \to +\infty$ and u_0(B phase) as $n \to -\infty$ and that the region in the vicinity of $n = 0$ forms a domian wall or soliton separating the B and A domains. This wall is analogous to that in a uniaxial antiferromagnet, with the order parameter changing sign over the wall thickness $d \equiv 2la$. We wish to find the energy E_s to form the soliton at rest, the width parameter l, the charge Q, and spin s of the soliton, as well as its effective mass M_s. Other quantities of interest are the spacial distributions of the soliton's spin and charge density, its interaction with charged impurities, and internal vibrational excitations of the soliton.

If one calculates straightforwardly the energy to create a soliton in a finite length of chain, a difficulty arises. Suppose the chain is initially in the A phase and a soliton is created so that the left-hand portion of the chain is in the B phase. The system increases its energy not only because of the increase of local energy in the vicinity of the soliton but also because the left-hand boundary of the chain terminates B-phase material rather than A-phase material. This end-effect energy shift is inconvenient since we want to treat the solitons as localizable elementary excitations. One scheme to eliminate the difficulty is to create an antisoliton ($\bar{S}$) followed by a soliton (S) so that the material goes from A to B to A as one moves from left to right along the chain. If S and $\bar{S}$ are widely separated they do not interact and the energy change is twice the soliton creation energy E_s.

To simplify the numerical work, we found it convenient to calculate the energy of a single soliton in a finite chain for various shapes of the wall. Since the end effect is independent of wall shape, a calculation of the absolute energy of $S + \bar{S}$ for any single wall width serves to fix the zero of soliton energy when calculating the energy of a single soliton in a finite chain. This is the procedure we use. Alternatively, one can calculate the end-effect energy analytically by determining the energy difference between an A- and B-phase end of a chain.

To determine the minimum energy configuration which approaches the perfect A and B phases as n goes to $+\infty$ and $-\infty$, respectively, we isolate a segment of the chain surrounding the soliton whose center is located at $n = 0$. Let the segment extend from $n = -\nu$ to $+\nu$. We decompose the full Born-Oppenheimer Hamiltonian H into

$$H = H_0 + \hat{V} \ , \tag{4.3}$$

where the zero-order Hamiltonian H_0 corresponds to perfect B-phase displacements for $n \leq -\nu$ and perfect A-phase displacements for $n \geq \nu$. The hopping is defined to be zero between groups in the segment $-\nu \leq n \leq \nu$. Therefore, the hopping integrals defining H_0 are

$$t^0_{n+1,n} = \begin{cases} t_0 - (-1)^{n-\nu} t_1, & n < -\nu \\ 0, & -\nu \leq n < \nu \\ t_0 + (-1)^{n-\nu} t_1, & n \geq \nu. \end{cases} \tag{4.4}$$

Here for convenience, we have taken ν to be odd. Physically, H_0 describes $2\nu - 1$ isolated atoms between the semi-infinite B and A chains. The perturbation $\hat{V}$ is the missing hopping in the isolated segment for any set of displacement order parameters $\{\psi_n\}$

$$-\hat{V}_{n,n+1} = -V_{n+1,n} = t_0 + (-1)^n \alpha(\psi_{n+1} + \psi_n) \quad -\nu \leq n < \nu \ . \tag{4.5}$$

The ψ_n's are to be varied so as to minimize the total system energy.

A convenient method for determining the ground-state energy shift ΔE of an extended system due to a localized perturbation $\hat{V}$ is the relation[23]

$$\Delta E = \frac{2}{\pi}\int_{-\infty}^{\mu} \mathrm{Im}\ln\det[1 - G^0(\omega)]\hat{V}\, d\omega \ . \quad (4.6)$$

G^0 is the Green function in the absence of $\hat{V}$, and μ is the chemical potential, which is zero for our system. This method has the advantage that one need not diagonalize H to determine ΔE. Also, the determinant has a size limited by the spacial extent of $\hat{V}$. In our case the determinant has dimension $2\nu+1$. We find good convergence for the soliton in $(CH)_x$ with $2\nu+1$ of order 41–61.

To evaluate Eq. (4.6) we must determine G^0. Since the H_0 hopping breaks the chain into three noninteracting segments

$$\begin{aligned} &A \quad n \geq \nu \ , \\ &S \quad -\nu < n < \nu \ , \\ &B \quad n \leq -\nu \ . \end{aligned} \quad (4.7)$$

G^0 is block diagonal in these segments. In S, one has

$$G^0_{nn'}(\omega) = (1/\omega)\delta_{n,n'}, \quad -\nu < n,n' < \nu \ . \quad (4.8)$$

To determine G^0 in A, we consider a perfect A-phase chain and place an infinite-site diagonal potential U on group $\nu-1$ so that the chain to the right of this site is uncoupled from site $\nu-1$ and thereby uncoupled from the rest of the chain. In segment A, G^0 satisfies

$$G^0_{nn'} = G^d_{nn'} + G^d_{n,\nu-1}UG^0_{\nu-1,n'} \ , \quad n,n' \geq \nu \ , \quad (4.9)$$

where G^d is given by Eq. (3.24). Taking the limit $U \to \infty$, one finds for the A segment

$$G^0_{nn'} = G^d_{nn'} - \frac{G^d_{n,\nu-1}G^d_{\nu-1,n'}}{G^d_{nn}} \ , \quad n,n' \geq \nu \ . \quad (4.10)$$

In the B segment, G^0 is determined in the same manner from a B-phase chain by placing an infinite potential on site $-\nu+1$,

$$G^0_{nn'} = \bar{G}^d_{nn'} - \frac{\bar{G}^d_{n,-\nu+1}\bar{G}^d_{-\nu+1,n'}}{G^d_{nn}} \ , \quad n,n' \leq -\nu \ . \quad (4.11)$$

where $\bar{G}^d$ is the Green's function for a B-phase chain, corresponding to $t_1 \to -t_1$ in the expression for G^d. We note that as a consequence of symmetry, one has the relation,

$$G^0_{nn'} = G^0_{-n',-n} \ . \quad (4.12)$$

The determinant in Eq. (4.6) is evaluated in the site representation. Since $\hat{V}$ is zero in segments A and B, only the boundary limits of G^0 in these segments enter, i.e., $G^0_{\nu\nu}$ and $G^0_{-\nu,-\nu}$. From Eqs. (4.10) and (4.11) one finds

$$\begin{aligned} G^0_{\nu\nu}(\omega) &= G^0_{-\nu,-\nu}(\omega) \\ &= G^d_{nn}(\omega) - \frac{[G^d_{n,n+1}(\omega)]^2}{G^d_{nn}(\omega)} \ , \end{aligned} \quad (4.13)$$

where G^d_{nn} and $G^d_{n,n+1}$ are given by Eqs. (3.25) and (3.27).

The integral in Eq. (4.6) was carried out numerically with the trial function

$$\psi_n = \begin{cases} u_0, & n \leq -\nu \\ -u_0\tanh(n/l), & \nu < n < \nu \\ -u_0, & n \geq \nu. \end{cases} \quad (4.14)$$

ΔE is plotted in Fig. 8 for three values of the energy gap $E_G = 1.0$, 1.4, and 2.0 eV. As discussed above, the zero of energy was shifted to give the correct answer for a widely separated soliton-antisoliton pair with $l = 1$.

For the value 1.4 eV, the soliton formation energy is $E_s \cong 0.42$ eV and the width parameters $l \simeq 7$. We have tried other trial functions with little change of energy and shape of the soliton. Thus, for $(CH)_x$ the wall is quite diffuse and one expects small lattice

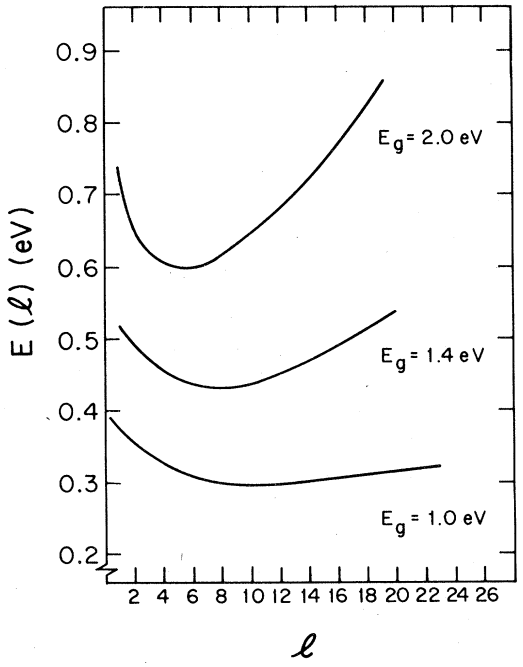

FIG. 8. Soliton energy $E(l)$ plotted as a function of an assumed half-width l for several values of the energy gap E_g.

periodicity effects in pinning the soliton. Preliminary calculations show that E_s varies by roughly 0.002 eV as the center of the soliton moves between lattice sites. This indicates that relatively free translation of the soliton would occur in an otherwise perfect lattice, down to temperatures on the order of 20–40 °K.

In passing we note that while the wall is diffuse, this does not imply that a Ginzburg-Landau-like theory involving a gradient expansion of the free-energy functional is appropriate. Rather, the wall thickness la is of the order of the nonlocality distance $\xi_0=\hbar v_f/\pi\Delta$ and a more accurate analysis, including nonlocality and umklapp processes, must be carried out, as we have done here.

To investigate the electronic structure of the soliton we have calculated the change in the density of states $\Delta\rho(E)$ due to the presence of the soliton. The results are plotted in Fig. 9 and show a single sharp state $\phi_0(n)$ at $E_0=0$, the gap center, for each spin orientation. Below, we derive the explicit form of $\phi_0(n)$. Since the total number of electronic states in the π band is conserved (i.e., independent of $\{\psi_n\}$), it follows that:

$$\int_{-\infty}^{\infty}\Delta\rho(E)\,dE=0\ . \tag{4.15}$$

From this relation and the fact that $\Delta\rho(E)$ is a symmetric function of E, it follows that the valence band has a deficit of one-half a state for each spin, as does the conduction band. Since the valence band is fully occupied both with and without the soliton, the valence band is missing a total of one electron in the presence of the soliton. It follows that in a neutral soliton the missing electron occupies the state ϕ_0. Note that the valence band remains spin paired while the electron in ϕ_0 is spin unpaired. Thus, *a neutral soliton has spin one-half.* As we discuss below, the low-energy-charged soliton states correspond to removing the unpaired electron from ϕ_0 or adding a second electron of opposite spin to ϕ_0. Therefore, *the spin of a charged soliton is zero.* In summary, one has

$$\begin{aligned} &Q_0=0,\quad s_0=\tfrac{1}{2},\\ &Q_\pm=\pm e,\quad s_\pm=0\ . \end{aligned} \tag{4.16}$$

It would appear that in forming a soliton we have violated Kramer's theorem, which requires that the spin of a system with an even number of electrons be an integer, and with an odd number be half an odd integer. Since the total number of electrons is conserved in creating a neutral soliton yet the soliton has spin $\frac{1}{2}$, a compensating spin must occur somewhere else in the system. The situation is clear for a ring of N CH groups, where N is very large compared to l. Because of the single-valuedness of the order parameter, a soliton S which separates B and A phases must be followed by an antisoliton $\bar{S}$ which separates A and B phases, as illustrated in Fig. 10. In this figure the order parameter is plotted radially, positive outside and negative inside the ring. If S and $\bar{S}$ are widely separated, their interaction is exponentially small and they are independent excitations. However if S and $\bar{S}$ are neutral, they each have spin $\frac{1}{2}$ and Kramers theorem is satisfied. This model also clarifies the counting of electronic states, since there must be an integer number of states in the valence band with and without S and $\bar{S}$. Since for each spin direction S and $\bar{S}$ each remove one-half of a state from the valence band, one complete state is removed by S plus $\bar{S}$, satisfying the integer-state counting rule. This result also holds for the conduction band. For a finite chain discussed above, a similar argument holds if S or $\bar{S}$ are created far from the chain ends and are themselves widely separated. If only S or $\bar{S}$ is created, it can be shown that an extra spin of one-

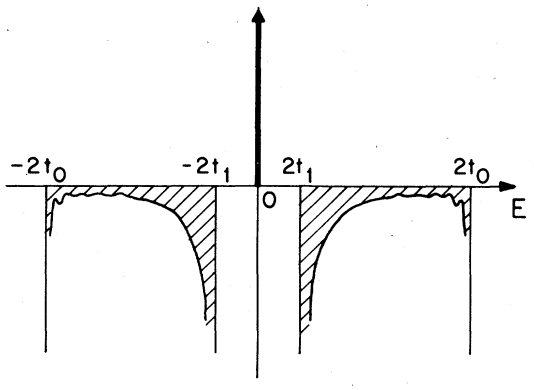

FIG. 9. Changes of density of states $\Delta\rho(E)$ due to the presence of a soliton. The gap center state gives a δ function of strength unity. This is compensated for by densities missing from the valence and conduction bands each integrating to one-half a state. In essence, the gap-center state is a nonbonding state between the bonding and antibonding bands.

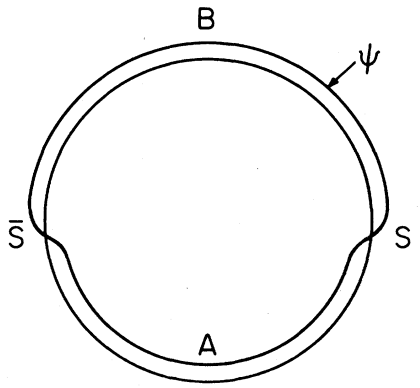

FIG. 10. Soliton S and antisoliton $\bar{S}$ occurring in a ring of $(CH)_x$. The order parameter ψ is plotted radially.

half is created or destroyed at a chain end, ensuring that Kramers theorem is satisfied.[24]

At each site n, the electron density missing from the valence band is exactly compensated by the density $|\phi_0(n)|^2$ of the unpaired electron. This can be proved as follows. For any configuration of the chain, the local density of states $\rho_{nn}(E)$ satisfies the sum rule

$$\int_{-\infty}^{\infty} \rho_{nn}(E)\, dE = 1 \ , \tag{4.17}$$

which follows from the completeness of the eigenstates of $H(\{\psi_n\})$. [Note Eq. (4.15) follows from Eq. (4.17) by summing on n.] Therefore the change of $\rho_{nn}(E)$ due to the presence of the soliton integrates to zero. Furthermore, $\Delta\rho_{nn}(E) = \Delta\rho_{nn}(-E)$, so that we find the local compensation sum rule

$$2\int_{-\infty}^{-\Delta} \Delta\rho_{nn}(E)\, dE + |\phi_0(n)|^2 = 0 \ , \tag{4.18}$$

which proves that the missing electron density in the valence band is exactly compensated at each site by the ϕ_0 electron density. Thus, a neutral soliton is both globally and locally charge neutral. An analogous relation of local charge compensation has been derived by Brazovskii[4] in the continuum model.

Since the energy of the system is the same if the occupancy of ϕ_0 is zero, one, or two, the width and energy of the soliton are identical for the three charge states $Q = 0, \pm e$. From this it follows that the charge distribution of the $Q = 0, \pm e$ soliton is given by $\pm e\,|\phi_0(n)|^2$.

$\Delta\rho_{nn}(E)$ for the valence band is shown in Fig. 11 for $n = 0$, 6, and 12, and for $n = 1$, 5, and 11 in Fig. 12. The smallness of $\Delta\rho_{nn}(E)$ for odd n is consistent with the fact that $|\phi_0(n)|^2$ vanishes for odd n, as we now demonstrate. Since $E_0 = 0$, the wave function

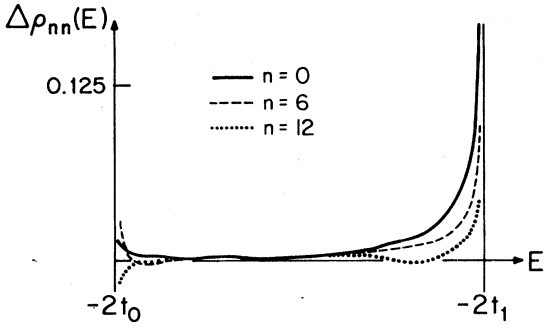

FIG. 11. Change in the local density of states $\Delta\rho_{nn}(E)$ due to the presence of a soliton, plotted for the valence-band region $-2t_0 < E < -2t_1$. Symmetry ensures $\Delta\rho_{nn}(E) = \Delta\rho_{nn}(-E)$, so the conduction- and valence-band changes are mirror symmetric about the gap center. Not shown is the δ function at the gap center of strength $|\phi_0(n)|^2$. Results for $n = 0$, 6, 12 are shown.

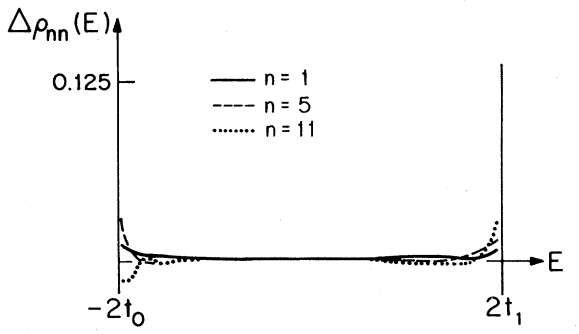

FIG. 12. Same as Fig. 11 except results for $n = 1$, 5, 11 are shown.

$\phi_0(n)$ of the gap center state satisfies

$$t_{n+1,n}\phi_0(n) + t_{n+1,n+2}\phi_0(n+2) = 0 \ , \tag{4.19}$$

where

$$\begin{aligned} t_{n+1,n} &= t_{n,n+1} \\ &= t_0 + (-1)^n \alpha(\psi_{n+1} + \psi_n) \end{aligned} \tag{4.20}$$

and ψ_n is given by Eq. (4.14). Since $\phi_0(n)$ for even and odd n are uncoupled, there are two linearly independent solutions, one of which decreases exponentially as $n \to \pm\infty$, while the other diverges and is not normalizable. If the soliton is centered on $n = 0, \pm 2, \ldots$ the normalizable state only involves even n, while it only involves odd n for a soliton centered at $\pm 1, \pm 3, \ldots$. The state is a linear combination of even and odd n if the soliton's center is between sites. In the present case, the soliton is centered on $n = 0$ and $\phi_0(n) = \phi_0(-n)$. For even n one finds

$$\begin{aligned} \phi_0(n+2) &= -\left(\frac{t_{n+1,n}}{t_{n+2,n+1}}\right)\phi_0(n) \\ &= \left(\frac{-t_{n+1,n}}{t_{n+2,n+1}}\right)\left(\frac{-t_{n-1,n-2}}{t_{n,n-1}}\right)\cdots\left(\frac{-t_{1,0}}{t_{2,1}}\right)\phi_0(0) \ . \end{aligned} \tag{4.21}$$

while $\phi_0(n) = 0$ for odd n. $\phi_0(0)$ is determined so that ϕ_0 is normalized to unity. $|\phi_0(n)|^2$ is plotted in Fig. 13, for $l = 7$ and $l = 5$, showing little variation with l. Roughly speaking, $\phi_0(n)$ behaves like a WKB state, tunneling through a barrier of height Δ and modulated by the zone-edge wave function for $k = \pm\pi/2\alpha$,

$$\phi_0(n) \cong \frac{1}{l}\,\mathrm{sech}\frac{n}{l}\cos\tfrac{1}{2}\pi n \ . \tag{4.22}$$

In passing we note that Coulomb interactions

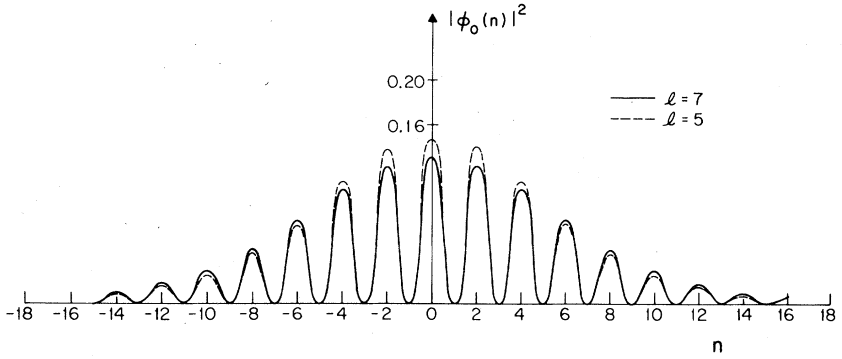

FIG. 13. Gap-center state probability density $|\phi_0(n)|^2$ plotted for a soliton centered on $n=0$. Two soliton widths $l=5$ and 7 are considered. By symmetry, $\phi_0(n)=0$ for odd n if the soliton is centered on even n.

between electrons split the ϕ_0 level for different occupancies in a nonintuitive fashion.[25]

The mass M_s of the soliton can be determined by calculating the energy of a slowly moving domain wall,

$$\psi_n(t)=u_0\tanh[(na-v_s t)/la] \ . \tag{4.23}$$

From time-reversal symmetry, any change in wall shape, e.g., l, must be of order v_s^2 and does not contribute to M_s for small v_s. Continuing to work within the adiabatic approximation, we find

$$\tfrac{1}{2}M_s v_s^2=\tfrac{1}{2}M\sum_n \dot{\psi}_n^2$$
$$=\frac{Mu_0^2 v_s^2}{2l^2a^2}\sum_n \operatorname{sech}^4\left(\frac{n}{l}\right) \ . \tag{4.24}$$

Therefore, using the parameters for $E_G=1.4$ eV one obtains,

$$M_s=\frac{4}{3l}\left(\frac{u_0}{a}\right)^2 M \simeq 6m_e$$

where m_e is the free electron mass. The small value of M_s is a consequence of the smallness of the dimerization length u_0 compared to the lattice spacing a. One would expect that the soliton would have high mobility because of its small mass, and it must be treated as a quantum particle.

V. DOPING EFFECTS

In the traditional semiconductor picture of doping, an impurity donates an electron (or hole) to the conduction (or valence) band of the solid and no structural change of the solid occurs. In $(CH)_x$, one must consider whether the state of lower energy is a free electron (or hole) as in the semiconductor picture, or a charged soliton ($Q=\pm e$). Choosing the center of the gap as the origin of energy, the minimum energy to inject an electron (or hole) is Δ, while the energy to make a charged soliton is E_s. Thus, if

$$E_s<\Delta \tag{5.1}$$

soliton doping occurs through the formation of charged solitons, while if

$$E_s>\Delta \tag{5.2}$$

semiconductor band doping occurs. For a range of gap sizes we found $E_s\sim 0.6\Delta$. Therefore, soliton doping is favored in $(CH)_x$-like systems. This result implies that for each donor (K, Na, etc.) or acceptor (Cl, AsF_5, etc.) which transfers an electron or a hole to the chain,[26] one charged soliton is formed. Since charged solitons have zero spin, no spin resonance or Curie-law susceptibility would be associated with the charge carriers, as is experimentally observed. One might ask, how is it possible to transport a single charge $+e$ without having spin transport. In essence, the charged soliton carries one missing electron, half of which is in the up-spin valence band and half in the down-spin valence band. This is accomplished by slightly deforming all of the states in the valence band so as to reduce locally the up- and down-spin electron density each by a total of half an electron in the vicinity of the soliton. Far from the soliton, the electron density returns precisely to its value without the soliton. For $Q=-e$, the soliton has two electrons spin paired in ϕ_0 and the missing electron density from the valence band is doubly compensated for by the ϕ_0 electrons.

Next we calculate the interaction energy of ΔE_l of a charged soliton $Q=\pm e$ interacting with an impurity of opposite sign of charge $Q'=\mp e$. For simplicity we assume the impurity to be a point charge located a distance d from the chain and centered at $n=0$. When the soliton is centered on site n_s, the Born-

Oppenheimer energy has the additional term

$$\Delta E_l = -\frac{e^2}{\epsilon}\sum_n \frac{|\phi_0(n-n_s)|^2}{[(na)^2+d^2]^{1/2}} \quad , \tag{5.3}$$

where we assume the interaction is screened by the macroscopic dielectric constant ϵ. For $E_G = 1.4$ eV and $\epsilon = 10$, one finds for $|x_s|/d < 1$,

$$\Delta E_l(x_s) = -E_b + \tfrac{1}{2}k_b x_s^2 + O(x_s^4) \quad , \tag{5.4}$$

where $x_s = n_s a$. One finds $E_b = 0.33$ eV and $k_b = 0.0029$ eV/Å^2 for $d = 2.0$ Å and 0.30 eV and 0.0028 eV/Å^2, respectively, for $d = 2.4$ Å. If the soliton is treated classically, the equilibrium binding energy is E_b, compared to a measured activation energy for conductivity in the dilute alloy $\Delta E_{\text{cond}} \cong 0.30$ eV.

For small amplitude motion of the soliton about the position of the charged impurity, one obtains the quantum of vibrational energy

$$\hbar\omega_s = \hbar(k_b/M_s)^{1/2} = \begin{cases} 0.06 \text{ eV}, & d = 2.0 \text{ Å} \\ 0.05 \text{ eV}, & d = 2.4 \text{ Å}. \end{cases} \tag{5.5}$$

Treating the soliton as a quantum particle, the zero-point motion reduces the equilibrium binding energy to $E_b - \frac{1}{2}\hbar\omega_s$.

In a more complete treatment of the soliton-impurity interaction, l must be allowed to vary to minimize the system energy since the Coulomb energy is reduced as l is decreased. In Fig. 14, $-E_b(l)$ for $x_s = 0$ is plotted as a function of l as calculated from Eq. (5.3) for $E_G = 1.4$ eV and $d = 2.4$ Å. Also plotted are $E_s(l)$ for the free soliton and $E_s(l) - E_b(l)$. For the bound soliton, the Coulomb attraction shrinks wall thickness to approximately $l = 5$ and increases the binding energy to $E_b = 0.32$ eV. The shifted vibrational quantum is $\hbar\omega_s = 0.07$ eV. The dipole oscillator strength of this excitation is large because it corresponds to a full electronic charge being excited.

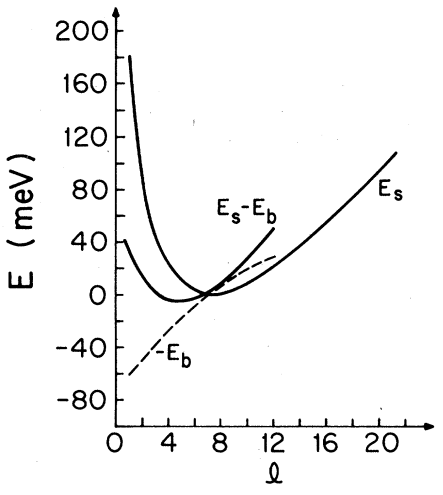

FIG. 14. Free-soliton energy E_s, the Coulomb energy of charged soliton-charged impurity interaction $-E_b$, and the sum $E_s - E_b$ are plotted as a function of the soliton width l. When bound to an impurity the soliton width decreases somewhat, although the binding energy changes relatively little due to this effect.

Another excitation mode of the soliton is the l or shape oscillation. If one writes

$$\psi_n(t) = u_0 \tanh\{na/[la + \delta(t)]\} \tag{5.6}$$

then an effective Hamiltonian can be written

$$H_l = \tfrac{1}{2}k_1\delta^2 + \tfrac{1}{2}M_1\dot{\delta}^2 \quad , \tag{5.7}$$

and

$$\hbar\omega_1 = \hbar(k_1/M_1)^{1/2} \quad . \tag{5.8}$$

The coefficients k_1 and M_1 are given by

$$k_1 = \frac{1}{a^2}\frac{\partial^2 E_s}{\partial l^2} \quad , \tag{5.9}$$

$$M_1 = \frac{Mu_0^2}{a^2 l^4}\sum_n n^2 \operatorname{sech}^4\left(\frac{n}{l}\right) \quad . \tag{5.10}$$

For $E_G = 1.4$ eV, and $l = 7$, $\hbar\omega_1 = 0.09$ eV. Infrared absorption experiments on doped $(CH)_x$ have been carried out by Fincher *et al.*[27] and phonon modes in the presence of a soliton have been treated by Mele and Rice.[28]

VI. COMPARISON WITH EXPERIMENT; CONCLUSION

The existence of paramagnetic defects in undoped *trans*-$(CH)_x$ is well established.[6–10] Isomerization of *cis*-films results in a spin resonance signal whose intensity grows with increasing *trans*-isomer content.[6] The results imply that the magnetic defects in *trans*-$(CH)_x$ are not due to impurities but are on the polymer chain and are induced by isomerization.

Goldberg *et al.*[7] suggested that the narrow room-temperature electron-spin resonance (ESR) in *trans*-$(CH)_x$ results from motional narrowing due to a mobile bond-alternation domain wall. Recent ESR studies[29] of $(CH)_x$ and $(CD)_x$ have demonstrated that the ESR linewidths are determined by the unresolved hyperfine splittings; the temperature dependences of the measured linewidths in *trans*-$(CH)_x$ and *trans*-$(CD)_x$ are consistent with the picture of a mobile defect. The mobility of the neutral defects has been confirmed through observation of the Overhauser effect in *trans*-$(CH)_x$ by Nechtshein *et al.*[16] However, they observed no such enhancement in *cis*-$(CH)_x$ (i.e., containing a small *trans* content), but rather the "solid-state" effect due to coupling to immobile electron spins. Thus the neutral defects induced by isomerization are highly mobile

only in the fully isomerized *trans*-$(CH)_x$ in agreement with the ESR studies. The spin resonance of the trapped immobile defects in the partially isomerized polymer has been used to obtain information on the spatial extent of the magnetic defect.[29] Analysis of the results implies a delocalization of the spin over a region with half-width of about seven lattice constants. Thus the theoretical description of these neutral defects (in the undoped polymer) as mobile solitons, with the unpaired spin spread over the extended domain wall, is in good agreement with all aspects of the experimental results.

Experimental studies of the doped polymer are also qualitatively consistent with the concept of doping through soliton formation. Light doping of $(CH)_x$ produces a dramatic increase in conductivity with no accompanying increase in Curie-law spin susceptibility.[8] It has been suggested[30] that this may be attributable to nonuniform clustering of dopants into metallic regions, resulting in a small Pauli, rather than Curie, magnetic susceptiblity. While such clustering may play a role at dopant concentrations approaching the semiconductor-metal transition (~ 1 mole%), complete clustering is unlikely especially at the lightest doping levels. Moreover, compensation of the charge carriers by many orders of magnitude in undoped *trans*-$(CH)_x$ produces no decrease in Curie-law intensity.[7] Thus the spins associated with the Curie law and the charges associated with the conductivity are apparently decoupled in the lightly doped regime. Furthermore the strength of the Curie-law contribution decreases[8,31] on doping consistent with the expected ionization of isomerization-induced neutral solitons upon doping.

We conclude that the solitons,[32] or bond-alternation domain walls, described theoretically in this paper appear to play a fundamental role in the properties of polyacetylene, especially at very light doping levels. However, detailed experimental studies are required, especially as a function of dopant concentration, to clarify the role of solitons in the doping mechanism and in the subsequent electrical transport.

ACKNOWLEDGMENTS

We would like to thank Dr. Sergi Brazovskii and Dr. Steven Kivelson for stimulating discussions, and Dr. J. Ritsko for permission to use the Imϵ data prior to publication. We are also indebted to Dr. David Campbell for an informative discussion on soliton-antisoliton collisions in ϕ^4 field theory. This work was supported in part by NSF Grant No. DMR 77-23420 and by NSF-MRL program under Grant No. DMR 76-80994.

---

*Address after January 1980: Dept. of Phys., Univ. of California, Santa Barbara, Calif. 93106.

[1]W. P. Su, J. R. Schrieffer, and A. J. Heeger, Phys. Rev. Lett. 42, 1698 (1979).
[2]M. J. Rice, Phys. Lett. A 71, 152 (1979).
[3]Hajime Takayama, Y. R. Lin-Liu, and Kazumi Maki, Phys. Rev. B 21, 2388 (1980).
[4]S. A. Brazovskii, JETP Lett. 28, 656 (1978); and private communication.
[5]B. Horovitz and J. A. Krumhansl, Solid State Commun. 26, 81 (1978).
[6]H. Shirakawa, T. Ito, and S. Ikeda, Die Macromol. Chem. 179, 1565 (1978).
[7]I. B. Goldberg, H. R. Crowe, P. R. Newman, A. J. Heeger, and A. G. MacDiarmid, J. Chem. Phys. 70, 1132 (1979).
[8]B. R. Weinberger, J. Kaufer, A. Pron, A. J. Heeger, and A. G. MacDiarmid, Phys. Rev. B 20, 223 (1979).
[9]A. Snow, P. Brant, and D. Weber, Polym. Lett. 17, 263 (1979).
[10]J. C. W. Chien, F. E. Karasz, G. Wnek, A. G. MacDiarmid, and A. J. Heeger, Polym. Lett. (in press).
[11]Y. W. Park, A. Denestein, C. K. Chiang, A. J. Heeger, and A. G. MacDiarmid, Solid State Commun. 29, 747 (1979); Y. W. Park, A. J. Heeger, M. A. Druy, and A. G. MacDiarmid, Phys. Rev. B (in press).
[12]S. Lefrant, L. S. Lichtman, H. Temkin, D. B. Fitchen, D. C. Miller, G. E. Whitehall, and J. M. Burlitch, Solid State Commun. 29, 191 (1979).
[13]I. Harada, M. Tasumi, H. Shirakawa, and S. Ikeda, Chem. Lett. (Jpn.) 12, 1411 (1978).
[14]C. Tric, J. Chem. Phys. 51, 4778 (1969).
[15]C. R. Fincher, Jr., D. L. Peebles, A. J. Heeger, M. A. Druy, Y. Matsumura, A. G. MacDiarmid, H. Shirakawa, and S. Ikeda, Solid State Commun. 27, 489 (1979); Y. W. Park, M. A. Druy, C. K. Chiang, A. J. Heeger, A. G. MacDiarmid, H. Shirakawa, and S. Ikeda, Polym. Lett. 17, 195 (1979). J. J. Ritsko, E. J. Mele, A. J. Heeger, A. G. MacDiarmid, and M. Ozaki (unpublished).
[16]M. Nechtschein, F. Devreux, R. L. Greene, T. C. Clarke, and G. B. Street, Phys. Rev. Lett. 44, 356 (1980).
[17]L. Salem, *The Molecular Orbital Theory of Conjugated Systems* (Benjamin, New York, 1966).
[18]R. E. Peierls, *Quantum Theory of Solids* (Clarendon, Oxford, 1955), p. 108.
[19]Y. Oshika, J. Phys. Soc. Jpn. 12, 1238, 1246 (1957).
[20]P. M. Grant and I. P. Batra, Solid State Commun. 29, 225 (1979).
[21]S. Hsu, A. Signorelli, G. Pez, and R. Baughman, J. Chem. Phys. 68, 5405 (1978); R. Baughman and S. Hsu, Poly. Lett. 17, 185 (1979).
[22]*Solitons and Condensed Matter Physics*, edited by A. R. Bishop and T. Schneider (Springer-Verlag, New York, 1978).
[23]T. L. Einstein and J. R. Schrieffer, Phys. Rev. B 7, 3629 (1973).
[24]W. P. Su (unpublished).
[25]J. R. Schrieffer (unpublished).
[26]For references see A. J. Heeger and A. G. MacDiarmid, in

Proceedings of the Dubrovnik Conference on Quasi-One-Dimensional Conductors, Lecture Notes in Physics 96, edited by S. Barisic (Springer-Verlag, Berlin-Heidelberg, 1979), p. 361; A. J. Heeger and A. G. MacDiarmid, in *NATO Conference Series VI: Materials Science* edited by W. Hatfield (Plenum, New York, 1979), p. 161. See also accompanying paper in this volume by A. G. MacDiarmid and A. J. Heeger for more details on chemical aspects of the problem.

[27]C. R. Fincher, Jr., M. Ozaki, A. J. Heeger, and A. G. MacDiarmid, Phys. Rev. B 19, 4140 (1979).

[28]E. J. Mele and M. J. Rice (unpublished).

[29]B. R. Weingberger, J. Kaufer, A. J. Heeger, and A. G. MacDiarmid, (unpublished).

[30]Y. Tomkiewicz, T. D. Schultz, H. B. Brown, T. C. Clarke, and G. B. Street, Phys. Rev. Lett. 43, 1532 (1979).

[31]P. Bernier, M. Rolland, M. Galtier, A. Montaner, M. Regis, M. Candille, and C. Benoit, J. Phys. Lett. 40, L297 (1979).

[32]While we have used the term soliton to refer to a shape-preserving nonlinear excitation in the absence of other such excitations, their integrity may be questioned when soliton-antisoliton collisions become important as their density increases. At present, little work has been done on soliton-antisoliton collisions in the coupled electron phonon model discussed above. However, judging from studies in the related problem of ϕ^4 field theory [T. R. Koehler (unpublished); C. Wingate (unpublished); B. S. Getmanov, JETP Lett. 24, 291 (1976); and A. E. Kudryavtsev, JETP Lett. 22, 82 (1975)], collisions between soliton and antisoliton rarely lead to their mutual annihilation. Rather, the excitations reflect approximately elastically or, for small relative velocity, can form a bound state. Investigation of this problem for the above Hamiltonian is being carried on by our group at present.